J. Fluid Mech. (1973), *vol.* 59, *part* 4, *pp.* 625–644
Printed in Great Britain

Periodic waves in shallow water

By P. J. BRYANT

Fluid Mechanics Research Institute, University of Essex, Colchester, Essex†

(Received 12 May 1972 and in revised form 12 December 1972)

An investigation is made into the evolution, from a sinusoidal initial wave train, of long periodic waves of small but finite amplitude propagating in one direction over water in a uniform channel. The spatially periodic surface displacement is expanded in a Fourier series with time-dependent coefficients. Equations for the Fourier coefficients are derived from three sources, namely the Korteweg–de Vries equation, the regularized long-wave equation proposed by Benjamin, Bona & Mahony (1972) and the relevant nonlinear boundary-value problem for Laplace's equation. Solutions are found by analytical and by numerical methods, and the three models of the system are compared. The surface displacement is found to take the form of an almost linear superposition of wave trains of the same wavelength as the initial wave train.

1. Introduction

Gravity waves on the surface of water in a uniform channel form a dispersive nonlinear system. Dispersive effects are least for waves that are long compared with the depth. The present investigation is concerned with gravity waves for which the effects of dispersion and nonlinearity are of comparable small magnitude, that is, waves of small but finite amplitude and moderate length.

An approximate governing equation for such waves propagating in one direction into water originally at rest was obtained by Korteweg & de Vries (1895). If x denotes the direction of wave propagation measured in units of the length scale in this direction, and the time t is measured in units of the corresponding linear long-wave time scale, their equation may be written as

$$\eta_t+\eta_x+\tfrac{3}{2}\epsilon\eta\eta_x+\tfrac{1}{6}\mu^2\eta_{xxx}=O(\epsilon^2,\epsilon\mu^2,\mu^4). \tag{1.1}$$

Here $\epsilon \ll 1$ is the ratio of a typical wave amplitude to the undisturbed depth, $\mu \ll 1$ is the ratio of the undisturbed depth to the x length scale, and $\epsilon\eta$ is the ratio of the surface displacement to the undisturbed depth. An alternative equation, namely

$$\eta_t+\eta_x+\tfrac{3}{2}\epsilon\eta\eta_x-\tfrac{1}{6}\mu^2\eta_{xxt}=O(\epsilon^2,\epsilon\mu^2,\mu^4), \tag{1.2}$$

has the same formal justification as the KdV equation (1.1), but has been shown by Benjamin *et al.* (1972) to have better mathematical properties.

An investigation is made here into the evolution in time, from a sinusoidal

† Permanent address: Mathematics Department, University of Canterbury, Christchurch, New Zealand.

initial wave train, of long spatially periodic waves of small but finite amplitude propagating in one direction over water of constant depth. The solutions are terminated at a time $t \sim \epsilon^{-2}$ at which the cumulative effect of the remainder in (1.1) and (1.2) may become significant. The solution is valid, to the same approximation, for the evolution in space of a temporally periodic wave train driven by a wave maker oscillating sinusoidally at one end of an open uniform channel, up to a distance $x \sim \epsilon^{-2}$ from the wave maker (Bona & Bryant 1973).

The spatially periodic function $\eta(x,t)$ is expanded in a Fourier series with time-dependent coefficients, which is substituted in turn into (1.1) and (1.2) to give two sets of equations for the Fourier coefficients. A third set of equations for the Fourier coefficients is found by substituting the Fourier series (together with an appropriate Fourier series for the velocity potential $\phi(x,y,t)$) into the nonlinear boundary conditions at the water surface. The same approximation in ϵ is made in the nonlinear boundary conditions as is made in the derivation of (1.1) and (1.2), but no explicit restriction is placed on μ.

The three sets of nonlinear equations for the Fourier coefficients have the same algebraic form, differing only in the values of the constant coefficients in the equations. Solutions are found, both analytically and numerically, in which no restriction is placed on the value of μ. Also, the two equations (1.1) and (1.2) are compared as models of long-wave equations as μ tends towards zero at fixed small ϵ.

Madsen, Mei & Savage (1970) described experiments by Galvin and presented the results of numerical calculations which are relevant to the present investigation. In their model, a wave maker at one end of a uniform channel was started smoothly from rest into sinusoidal motion. It was found in Galvin's experiments that, for $\epsilon/\mu^2 < \frac{1}{8}$ (in the present notation), the wave train remains nearly sinusoidal for a long distance from the wave maker; that, as ϵ/μ^2 increases, secondary crests appear sooner and in greater numbers; and that wave breaking occurs when $\epsilon/\mu^2 > 2{\cdot}5$. They presented a numerical solution for the case $\epsilon = \frac{1}{4}$, $\mu = \frac{1}{8}\pi$ and $\epsilon/\mu^2 = 16/\pi^2$, up to a distance $6\frac{1}{4}$ wavelengths from the wave maker and time 11 periods from rest. They interpreted the motion between the front of the wave train and the wave maker as being that of two cnoidal wave trains interacting nearly linearly with each other. Their solution is discussed in § 7.

Vliegenthart (1971) developed a numerical scheme for solving the initial-value problem for the KdV equation, choosing as one example an initial sinusoidal wave train. In the present notation, his solution is for the case $\epsilon = \frac{1}{15}$, $\mu = (0{\cdot}06)^{\frac{1}{2}}\pi$ and $\epsilon/\mu^2 \doteq 0{\cdot}11$. He found that the initial solution is approximately repeated, apart from a phase shift, after a time 1·84 wave periods from the initial instant. His solution is compared in § 7 with an analytical solution for the same set of parameters.

Kim & Hanratty (1971) presented experimental results and numerical calculations on the capillary–gravity wave trains generated by a sinusoidally moving wave maker at one end of a uniform shallow channel of water. Most of their results lie in the range $0{\cdot}1 < \epsilon/\mu^2 < 0{\cdot}2$. It is difficult to compare their results with Vliegenthart's solution or with the present solutions because dissipation is significant at the wave frequencies they used. Zabusky & Galvin (1971) compared

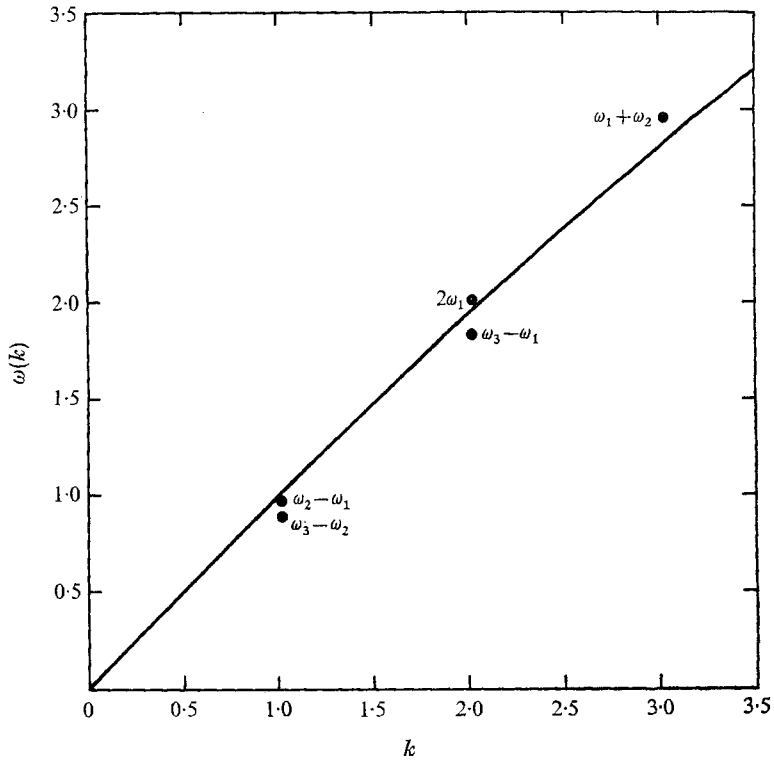

FIGURE 1. Dispersion relation when $\mu = \sqrt{0{\cdot}05}$.

laboratory measurements of periodic wave trains with numerical solutions o the KdV equation. Measurements of a wave train at the first station in a water channel were taken to be the initial conditions for comparison between calculations and measurements at the second station.

2. The principle of near-resonance

The dispersion relation for long gravity waves of infinitesimal amplitude propagating over water of uniform depth is

$$\begin{aligned}\omega(k) &= (k/\mu \tanh k\mu)^{\frac{1}{2}} \\ &= k(1-\tfrac{1}{6}(k\mu)^2+O(k\mu)^4),\end{aligned} \tag{2.1}$$

where the angular frequency ω is measured in units of the inverse time scale and the wavenumber k is measured in units of the inverse horizontal length scale. The horizontal length scale is chosen so that $k = 1$ for the initial sinusoidal wave train, that is,

$$\eta(x, 0) = \cos x.$$

(The reason for this choice is that it makes the derivatives of $\eta(x, 0)$ of the same magnitude as $\eta(x, 0)$, which is not the case when the wavelength is chosen as the length scale.) Equation (2.1) with $\mu = \sqrt{0{\cdot}05}$ is plotted in figure 1. The angular frequency of the kth wave mode, $k = 1, 2, \ldots$, is denoted by ω_k.

Consider now the generation of the second and higher harmonics by the nonlinear interaction whose first approximation is the nonlinear term of (1.1). The interaction of the first harmonic with itself generates a harmonic with wavenumber 2 and frequency $2\omega_1$. The natural harmonic of wavenumber 2 has a frequency ω_2, where from (2.1)

$$\omega_2 = 2\omega_1 - \mu^2 + O(\mu^4).$$

Hence the nonlinear interaction of the first harmonic with itself when $\mu^2 \ll 1$ causes *near-resonant* growth of the second harmonic, the maximum amplitude of the second harmonic being estimated as (equation (5.2))

$$\epsilon/(2\omega_1 - \omega_2) \sim \epsilon/\mu^2 \sim 1.$$

The maximum amplitude of the second and higher harmonics cannot exceed 1 since all the energy comes from the first harmonic. The important property is that, when $\mu^2 \ll 1$, the maximum amplitude of the second harmonic is not simply a fraction ϵ ($\ll 1$) of that of the first harmonic, but may rise to a value comparable with that of the first harmonic.

The interaction of the first harmonic with the second harmonic generates one harmonic of wavenumber 1 and frequency $\omega_2 - \omega_1$, and a second of wavenumber 3 and frequency $\omega_2 + \omega_1$, where

$$\omega_1 = \omega_2 - \omega_1 + \mu^2 + O(\mu^4)$$

and

$$\omega_3 = \omega_2 + \omega_1 - 3\mu^2 + O(\mu^4).$$

Hence the difference interaction causes near-resonant modification of the first harmonic, while the sum interaction causes near-resonant growth of the third harmonic, its maximum amplitude being estimated as (equation (5.5))

$$\epsilon^2/(2\omega_1 - \omega_2)(\omega_1 + \omega_2 - \omega_3) \sim \tfrac{1}{3}(\epsilon/\mu^2)^2.$$

Similar interactions occur between all harmonics present, although the interactions are weaker for the higher harmonics because they are further from resonance. The possibility exists, therefore, that the evolution of a wave system, such as that considered here, may be dominated by the near-resonant interactions between the lower harmonics composing it. This property is advanced later as the reason for the persistence of a nearly periodic time structure in all solutions of the present wave system.

3. Equations for the Fourier amplitudes

The spatially periodic surface displacement $\eta(x, t)$ is expanded in the Fourier series

$$\eta(x,t) = \frac{1}{2}\sum_{k=1}^{\infty} (A_k(t) \exp ik(x-t) + A_k^*(t) \exp -ik(x-t)) \tag{3.1}$$

$$= \frac{1}{2}\sum_{k=1}^{\infty} (B_k(t) \exp i(kx - \omega_k t) + B_k^*(t) \exp -i(kx - \omega_k t)) \tag{3.2}$$

(* denotes a complex conjugate), where

$$B_k(t)\exp -i\omega_k t = A_k(t)\exp -ikt \quad \text{for all } k,$$

and

$$A_1(0) = 1, \quad A_k(0) = 0 \quad \text{for} \quad k > 1.$$

Each of the three sets of equations for the Fourier amplitudes is of the form

$$A_k'(t) - i\mu^2 P_k A_k(t) = -i\epsilon \sum_{l=1}^{\frac{1}{2}(k-1),\frac{1}{2}k} S_{kl} A_l A_{k-l} - i\epsilon \sum_{l=1}^{\infty} R_{kl} A_l^* A_{k+l} + O(\epsilon^2). \quad (3.3)$$

The set of coefficients derived from the KdV equation (1.1) is

$$\left.\begin{aligned} P_k &= \tfrac{1}{6}k^3, \\ S_{kl} &= \begin{cases} \tfrac{3}{4}k, & l \neq \tfrac{1}{2}k, \\ \tfrac{3}{8}k, & l = \tfrac{1}{2}k, \end{cases} \\ R_{kl} &= \tfrac{3}{4}k. \end{aligned}\right\} \quad (3.4)$$

The set of coefficients for the BBM equation (1.2) is

$$\left.\begin{aligned} P_k &= \tfrac{1}{6}k^3/(1+\tfrac{1}{6}k^2\mu^2), \\ S_{kl} &= \begin{cases} \tfrac{3}{4}k/(1+\tfrac{1}{6}k^2\mu^2), & l \neq \tfrac{1}{2}k, \\ \tfrac{3}{8}k/(1+\tfrac{1}{6}k^2\mu^2), & l = \tfrac{1}{2}k, \end{cases} \\ R_{kl} &= \tfrac{3}{4}k/(1+\tfrac{1}{6}k^2\mu^2). \end{aligned}\right\} \quad (3.5)$$

The set of coefficients derived without restriction on μ is

$$\left.\begin{aligned} P_k &= (k-\omega_k)/\mu^2, \\ S_{kl} &= \begin{cases} R(k,-l,k-l,\omega_k,-\omega_l,\omega_{k-l},\mu), & l \neq \tfrac{1}{2}k, \\ \tfrac{1}{2}R(k,-l,k-l,\omega_k,-\omega_l,\omega_{k-l},\mu), & l = \tfrac{1}{2}k. \end{cases} \\ R_{kl} &= \frac{(\omega_{k+l}-\omega_l)(l\omega_{k+l}+(k+l)\omega_l)k+\omega_k^2 l(k+l)}{2\omega_l\omega_{k+l}(\omega_k+\omega_{k+l}-\omega_l)} - \mu^2\frac{\omega_k^2(\omega_l^2-\omega_l\omega_{k+l}+\omega_{k+l}^2)}{2(\omega_k+\omega_{k+l}-\omega_l)}, \\ &= R(k,l,k+l,\omega_k,\omega_l,\omega_{k+l},\mu \end{aligned}\right\} \quad (3.6)$$

The derivation of the third set is now summarized.

The governing equation for an irrotational motion bounded by a fixed surface $y = -1$ and free surface $y = \epsilon\eta$ may be written, without restriction on μ, as

$$\phi_{xx} + (1/\mu^2)\phi_{yy} = 0, \quad (3.7a)$$

$$\phi_y = 0 \quad \text{on} \quad y = -1, \quad (3.7b)$$

$$\eta_t - (1/\mu^2)\phi_y = \epsilon(\phi_t\phi_x)_x + O(\epsilon^2) \quad \text{on} \quad y = 0, \quad (3.7c)$$

$$\eta + \phi_t = \epsilon(-\tfrac{1}{2}\phi_x^2 - \tfrac{1}{2}(1/\mu^2)\phi_y^2 + \phi_t\phi_{yt}) + O(\epsilon^2) \quad \text{on} \quad y = 0. \quad (3.7d)$$

The Fourier series expansion of $\phi(x,y,t)$ that is compatible with the expansion (3.2) and satisfies (3.7*a*, *b*) is

$$\phi(x,y,t) = -\gamma(t) + \frac{1}{2}\sum_{k=1}^{\infty}(C_k(t)\exp i(kx-\omega_k t) + C_k^*(t)\exp -i(kx-\omega_k t))\cosh\mu k(1+y)/\cosh\mu k. \quad (3.8)$$

It is noted, from the linear theory, that $\gamma'(t)$, $B_k'(t)$ and $C_k'(t)$ are all $O(\epsilon)$.

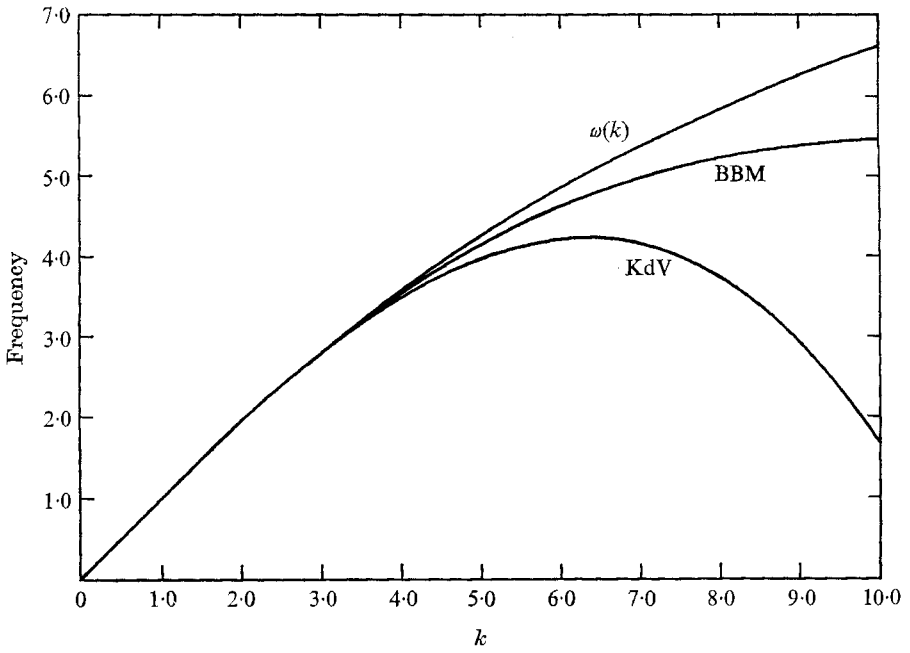

FIGURE 2. Dispersion relations for the three models when $\mu = \sqrt{0{\cdot}05}$.

When the Fourier expansions (3.2) and (3.8) are substituted into (3.7c, d), the elimination of $C_k(t)$ leaves

$$B_k'' - 2i\omega_k B_k' = -\epsilon \sum_{l=1}^{\frac{1}{2}(k-1),\frac{1}{2}k} (\omega_l + \omega_{k-l} + \omega_k) S_{kl} B_l B_{k-l} \exp -i(\omega_l + \omega_{k-l} - \omega_k) t$$
$$- \epsilon \sum_{l=1}^{\infty} (\omega_l + \omega_{k+l} - \omega_l) R_{kl} B_l^* B_{k+l} \exp i(\omega_l + \omega_k - \omega_{k+l}) t + O(\epsilon^2),$$

where S_{kl} and R_{kl} are given by equations (3.6). Multiplying this equation by $\exp(-2i\omega_k t)$ and integrating, we obtain

$$B_k' = -i\epsilon \sum_{l=1}^{\frac{1}{2}(k-1),\frac{1}{2}k} S_{kl} B_l B_{k-l} \exp -i(\omega_l + \omega_{k-l} - \omega_k) t$$
$$- i\epsilon \sum_{l=1}^{\infty} R_{kl} B_l^* B_{k+l} \exp i(\omega_l + \omega_k - \omega_{k+l}) t + O(\epsilon^2).$$

The constant of integration is put equal to zero because it represents a backward-propagating wave. When B_k is replaced by A_k, the set of equations (3.3) with the set of coefficients (3.6) is obtained.

4. Comparison of the models

Equations (1.1) and (1.2) are tested now as models of long-wave systems by comparing the three sets of coefficients (3.4), (3.5) and (3.6). Many of the differences between the solutions may be traced back to differences between the sets of coefficients.

The coefficient $\mu^2 P_k$ is the frequency of the kth harmonic relative to a frame of reference moving with unit velocity. The three expressions for the frequency of the kth harmonic relative to a stationary frame of reference are

$$k - \tfrac{1}{6}\mu^2 k^3 \quad \text{(KdV)},$$

$$k/(1 + \tfrac{1}{6}\mu^2 k^2) \quad \text{(BBM)}$$

and

$$\omega(k) = (k/\mu \tanh k\mu)^{\frac{1}{2}} \quad (\mu - \text{exact}).$$

The three expressions are sketched in figure 2 for $\mu = \sqrt{0{\cdot}05}$. It can be seen that they nearly coincide for $k\mu < 1$ ($k < 4{\cdot}5$), as is expected from the expansion of (2.1), but they diverge for $k\mu > 1$.

The KdV expression is very unsatisfactory for large k, since the frequency, phase velocity and group velocity all become large and negative. This behaviour causes the coefficient P_k to become large compared with 1, or equivalently, causes the interactions to be further from resonance. The amplitudes of the higher harmonics are therefore less than they should be, and the convergence of the Fourier series is assisted. This property also has the unfortunate effect in many numerical solutions that higher harmonics generated randomly by round-off errors may distort the solution, unless they are damped artificially. This difficulty does not arise here with the truncated Fourier series.

The BBM expression for the frequency provides a closer approximation to the μ-exact expression at large k, as was pointed out by the proposers of the BBM equation (1.2). The phase velocity and the group velocity tend towards zero as k becomes large compared with 1 with both the BBM and the μ-exact expressions.

The KdV expressions for R_{kl} and S_{kl}, which are independent of μ, are equal to the limit as $\mu \to 0$ of both the BBM and the μ-exact expressions for R_{kl} and S_{kl}. As μ increases from zero, the μ-exact expressions for R_{kl} and S_{kl} decrease to a minimum, and then increase asymptotically as $\sqrt{\mu}$. For the applicable range of μ and values of k and l, the KdV expressions for S_{kl} and R_{kl} are much less of an overestimate of their μ-exact counterparts than is the KdV expression for P_k an overestimate of its μ-exact counterpart.

The BBM expressions for R_{kl} and S_{kl} decrease monotonically towards zero as μ increases from zero. Over the applicable range of μ, they provide a good fit with the μ-exact expressions for the smaller values of k and l (for example, the two expressions for S_{21} are almost identical for $\mu < 1$), but for the larger values of k and l they underestimate the μ-exact expressions. This property makes the amplitudes of the higher harmonics less than they should be, and therefore assists in the convergence of the Fourier series.

In calculations on the present wave system, using each of the three sets of coefficients (3.4), (3.5) and (3.6) in turn, only quantitative differences were found between the solutions obtained. The KdV and BBM Fourier series both converge more rapidly than the μ-exact Fourier series, for the reasons outlined above. The BBM solutions are closer than the KdV solutions to the μ-exact solutions because the BBM coefficients are closer, in general, than the KdV coefficients to the μ-exact coefficients. This might by itself be considered sufficient reason to prefer the BBM model to the KdV model. For most numerical

solutions, the BBM model is decidedly preferable to the KdV model because it avoids the troublesome side-effects associated with the KdV dispersion relation.

5. Analytical solutions

The second and higher harmonics are generated by near-resonant nonlinear interactions. The higher the harmonic, the less effective are the near-resonant interactions generating it and subsequently modifying it. It can be expected therefore, and is found to be true, that the maximum amplitudes of the harmonics form a descending positive sequence from the value 1 for the first harmonic. A solution of the system (3.3), valid up to a given time with a given accuracy, is described by the Fourier series (3.1) truncated at the lowest harmonic whose maximum amplitude is less than an arbitrary small magnitude. The accuracy of such a solution may be tested by comparing it with the solutions obtained by terminating the Fourier series at higher harmonics.

The set $\mathscr{S}_n$ of equations contains those equations of the system (3.3) in which all the sum terms (the S_{kl} summation) are retained when the Fourier series (3.1) is terminated at the nth harmonic in the nonlinear terms. Consider now the sets of equations $\mathscr{S}_1$, $\mathscr{S}_2$ and $\mathscr{S}_3$ with the object of solving each and of finding for each the range of validity of μ for given small ϵ.

The set $\mathscr{S}_1$ is

$$\left.\begin{aligned} A_1' - i\mu^2 P_1 A_1 &= 0, \\ A_2' - i\mu^2 P_2 A_2 &= -i\epsilon S_{21} A_1^2, \end{aligned}\right\} \tag{5.1}$$

with the solution

$$\left.\begin{aligned} A_1 &= \exp i\mu^2 P_1 t, \\ A_2 &= \frac{\epsilon S_{21}}{\mu^2(P_2 - 2P_1)} (\exp 2i\mu^2 P_1 t - \exp i\mu^2 P_2 t) \\ &= \frac{2\epsilon S_{21}}{2\omega_1 - \omega_2} \sin(\omega_1 - \tfrac{1}{2}\omega_2) t \exp[i(2 - \omega_1 - \tfrac{1}{2}\omega_2) t - \tfrac{1}{2} i\pi]. \end{aligned}\right\} \tag{5.2}$$

$|A_2|$ is periodic with angular frequency $2\omega_1 - \omega_2$ and maximum amplitude $2\epsilon S_{21}/(2\omega_1 - \omega_2)$. Comparison of the set $\mathscr{S}_1$ with the set $\mathscr{S}_2$ (equations (5.3)) shows that the solution (5.2) is valid when $|A_1 A_2| \sim \epsilon$, that is, when $\mu \sim 1$ or $2\omega_1 - \omega_2 \sim 1$. Neither the KdV equation nor the BBM equation is a satisfactory model for this range of μ.

The set $\mathscr{S}_2$ is

$$\left.\begin{aligned} A_1' - i\mu^2 P_1 A_1 &= -i\epsilon R_{11} A_1^* A_2, \\ A_2' - i\mu^2 P_2 A_2 &= -i\epsilon S_{21} A_1^2, \\ A_3' - i\mu^2 P_3 A_3 &= -i\epsilon S_{31} A_1 A_2. \end{aligned}\right\} \tag{5.3}$$

The first two equations of $\mathscr{S}_2$ satisfy the energy conservation relation

$$S_{21} A_1 A_1^* + R_{11} A_2 A_2^* = S_{21}.$$

The solution of $\mathscr{S}_2$ is

$$\left.\begin{aligned} |A_1| &= [1-R_{11}/S_{21}\alpha^2\,\mathrm{sn}^2\,(S_{21}\epsilon t/\alpha)]^{\frac{1}{2}},\\ |A_2| &= \alpha\,\mathrm{sn}\,(S_{21}\epsilon t/\alpha), \quad \mathrm{mod}\, R_{11}\alpha^2/S_{21},\\ d(\arg A_1)/dt &= \mu^2[P_1-(\tfrac{1}{2}P_2-P_1)\,|A_2/A_1|^2\,R_{11}/S_{21}],\\ d(\arg A_2)/dt &= \mu^2(P_1+\tfrac{1}{2}P_2), \quad |A_2| \neq 0,\\ [\arg A_2] &= \pi \quad \text{at} \quad |A_2| = 0,\\ A_3 &= -i\epsilon S_{31}\int_0^t A_1(\tau)\,A_2(\tau)\exp i\mu^2P_3(t-\tau)\,d\tau, \end{aligned}\right\} \tag{5.4}$$

where

$$\alpha = \left(\frac{S_{21}}{R_{11}}+\frac{\mu^4(P_2-2P_1)^2}{16\epsilon^2R_{11}^2}\right)^{\frac{1}{2}}-\frac{\mu^2(P_2-2P_1)}{4\epsilon R_{11}}.$$

$|A_1|$ and $|A_2|$ are both strictly periodic with period $2\alpha/\epsilon S_{21}F_1(R_{11}\alpha^2/S_{21})$, where F_1 is the complete elliptic integral of the first kind. The expansions of the period and maximum amplitude of $|A_2|$ in powers of ϵ/μ^2 are

$$\text{period} = [2\pi/(\mu^2(P_2-2P_1))]\,(1+O(\epsilon/\mu^2)^2),$$
$$\alpha = [2\epsilon S_{21}/(\mu^2(P_2-2P_1))]\,(1+O(\epsilon/\mu^2)^2),$$

which suggests that the solution is valid when $(\epsilon/\mu^2)^2 \sim \epsilon$. This range of μ is confirmed as follows.

The $\mathscr{S}_1$ solutions for A_1 and A_2 are substituted into the $\mathscr{S}_2$ convolution for A_3 to give the first approximation

$$A_3 = (\epsilon/\mu^2)^2 S_{21}S_{31}\left(\frac{\exp 3i\mu^2P_1t}{(P_2-2P_1)\,(P_3-3P_1)}-\frac{\exp i\mu^2(P_1+P_2)\,t}{(P_2-2P_1)\,(P_3-P_1-P_2)}+\frac{\exp i\mu^2P_3t}{(P_3-3P_1)\,(P_3-P_1-P_2)}\right). \tag{5.5}$$

Comparison of the set $\mathscr{S}_2$ with the set $\mathscr{S}_3$ (equations (5.6)) shows that the solution (5.4) is valid when $|A_1A_3| \sim \epsilon$, that is, $(\epsilon/\mu^2)^2 \sim \epsilon$ or $\mu^4 \sim \epsilon$. The KdV and BBM equations are unsatisfactory models for this range of μ, since terms $O(\mu^4)$ in the remainders of these equations are of the same magnitude as the terms $O(\epsilon)$ included in the equations. It is an unsatisfactory approximation, therefore, to terminate a Fourier series expansion at only two terms when using either the KdV equation or the BBM equation as a model of a long-wave system.

The set $\mathscr{S}_3$ is

$$\left.\begin{aligned} A_1'-i\mu^2P_1A_1 &= -i\epsilon R_{11}A_1^*A_2-i\epsilon R_{12}A_2^*A_3,\\ A_2'-i\mu^2P_2A_2 &= -i\epsilon S_{21}A_1^2-i\epsilon R_{21}A_1^*A_3,\\ A_3'-i\mu^2P_3A_3 &= -i\epsilon S_{31}A_1A_2,\\ A_4'-i\mu^2P_4A_4 &= -i\epsilon S_{41}A_1A_3-i\epsilon S_{42}A_2^2. \end{aligned}\right\} \tag{5.6}$$

The first three of these equations satisfy the energy conservation relation

$$S_{21}S_{31}A_1A_1^*+R_{11}S_{31}A_2A_2^*+(R_{12}S_{21}+R_{11}R_{21})\,A_3A_3^* = S_{21}S_{31}.$$

It has not been possible to find an explicit analytical solution to the set $\mathscr{S}_3$. Instead, a first approximation is found by using the previous solutions to the sets $\mathscr{S}_1$ and $\mathscr{S}_2$.

The final term of each of the first two equations of the set $\mathscr{S}_3$ is rewritten, using (5.2) and (5.5), to give

$$\left.\begin{aligned} &A_1' - i\mu^2\left(P_1 - \frac{(\epsilon/\mu^2)^4 R_{12}S_{21}^2 S_{31}}{(P_2-2P_1)^2(P_3-3P_1)}\right)A_1 \\ &\quad = -i\epsilon\left(R_{11} + \frac{(\epsilon/\mu^2)^2 R_{12}S_{21}S_{31}}{(P_2-2P_1)(P_3-P_1-P_2)}\right)A_1^* A_2 + i\epsilon O(\epsilon/\mu^2)^3, \\ &A_2' - i\mu^2\left(P_2 - \frac{(\epsilon/\mu^2)^2 R_{21}S_{31}}{P_3-P_1-P_2}\right)A_2 \\ &\quad = -i\epsilon\left(S_{21} - \frac{(\epsilon/\mu^2)^2 S_{21}R_{21}S_{31}}{(P_3-3P_1)(P_3-P_1-P_2)}\right)A_1^2 \\ &\qquad -i\epsilon\frac{(\epsilon/\mu^2)^2 S_{21}R_{21}S_{31}}{(P_3-3P_1)(P_3-P_1-P_2)}\exp i\mu^2(P_3-P_1)t. \end{aligned}\right\} \quad (5.7)$$

The near-resonant contribution of each of the final terms of the original equations appears as a small frequency shift in the second term of each of the rewritten equations.

The solution of (5.7) oscillates closely about the $\mathscr{S}_2$ solution (equations (5.4)) with the coefficients taking their modified values. $|A_1|$ and $|A_2|$ are nearly periodic. It may be deduced by the same arguments as before that this solution is valid when $(\epsilon/\mu^2)^3 \sim \epsilon$, that is, when $\mu^3 \sim \epsilon$.

Although it appears to be possible to solve the set $\mathscr{S}_4$ by successive approximation in powers of ϵ/μ^2, the calculations become formidably long.

The analytical solutions above are valid only for values of ϵ/μ^2 small compared with 1. The technique of solution fails for values of ϵ/μ^2 comparable or large compared with 1, that is, for the more strongly nonlinear cases, because the number of harmonics becomes too large for analytical manipulation.

6. Numerical solutions

Each set $\mathscr{S}_n$ of equations may be integrated numerically stepwise in time from the given initial values. The numerical scheme used is stable for the linear terms of each equation. The kth equation of $\mathscr{S}_n$ is replaced by the difference equation

$$(A_k(t+\Delta t) - A_k(t-\Delta t))/2\Delta t - \tfrac{1}{2}i\mu^2 P_k(A_k(t+\Delta t) + A_k(t-\Delta t) = -i\epsilon F_k(A(t)) \quad (k = 1, 2, \ldots, n+1), \quad (6.1)$$

where F_k represents the nonlinear operator. The step size was usually chosen to be $\epsilon\Delta t = \frac{1}{200}\pi$, or $\epsilon\Delta t = 0{\cdot}01$.

The nonlinear right-hand side of (6.1) was usually evaluated at time t when calculating A_k at time $t+\Delta t$. It was noticed in cases of marginal numerical stability that stability is improved if use is made of $A_k(t+\Delta t)$ in calculations subsequent to its determination. This was done by replacing $A_l(t)$ by

$$\tfrac{1}{2}(A_l(t-\Delta t) + A_l(t+\Delta t)) \quad (l = 1, 2, \ldots, k-1)$$

in the right-hand side of (6.1).

The method of solution for each pair of values of ϵ and μ^2 is as follows. The Fourier series is terminated, by trial and error, at the lowest wave mode whose maximum magnitude is less than 10^{-2}. This solution is then compared with the solution obtained by including one more wave mode in the Fourier series. If the maximum difference between the solutions is less than 10^{-2} in magnitude, the first solution is taken to be the solution for this ϵ and μ^2. For some examples using the μ-exact coefficients, the maximum difference exceeds 10^{-2}, so further wave modes are added to the Fourier series until the difference between consecutive solutions is less than 10^{-2}. The penultimate solution is then taken as the solution for this ϵ and μ.

The form of the solutions is one of intersecting wave trains of wavelength 2π. The greater the value of ϵ/μ^2, the greater the number of wave trains present. The period of $|A_1|$ is the time scale for the nearly periodic time structure of the wave trains. At a time equal to this period after the initial instant, each crest of the primary wave train intersects with the crest of the secondary wave train that started 2π behind it, together with the crest of the tertiary wave train that started 4π behind it, and so on. At a time equal to half this period after the initial instant, each crest of the primary wave train intersects with the crest of the tertiary wave train that started 2π behind it, and so on. At each intersection, the crest of each of the intersecting wave trains is advanced in phase, the discontinuity being greater for the lower order wave train. The crests move with nearly constant phase velocity between intersections. In all examples considered, the nearly periodic time structure persisted over the whole range of integration.

This property raises the question as to whether there exist shallow-water solutions (other than a single cnoidal wave) which are strictly periodic in time as well as in space. Do the present solutions tend asymptotically towards a strictly periodic state, or is it possible to choose the initial conditions appropriately so that the solution is strictly periodic? There is no good reason emerging from the present analysis why this should not be true.

7. Examples

The first five examples cover the range $\frac{1}{4} \leqslant \epsilon/\mu^2 \leqslant 4$ at fixed $\epsilon = \frac{1}{20}$. The value of ϵ is chosen to be small to make the error $O(\epsilon^2)$ in the equations also small. The range of integration in each case is $0 \leqslant \epsilon t \leqslant 5\pi$, that is, 50 wave periods (according to the linear theory) from the initial instant.

The sets of three parameter values below refer to the KdV, BBM and μ-exact equations, in that order.

$$\epsilon = \tfrac{1}{20}, \quad \mu^2 = \tfrac{1}{5}, \quad \epsilon/\mu^2 = \tfrac{1}{4}.$$

The number of harmonics in the Fourier series is 4 in each case; the period of $|A_1|$ is 4·7, 5·45 or 6·15 wave periods; the maximum value of $|A_2|$ is 0·35, 0·35 or 0·39; and the phase velocity of the primary wave trains is 0·95 in each case between phase discontinuities at their intersections with the secondary wave trains. The definition of the secondary wave trains is not sufficiently clear to measure their phase velocity. The amplitudes $|A_1|$, $|A_2|$ and $|A_3|$ for the μ-exact

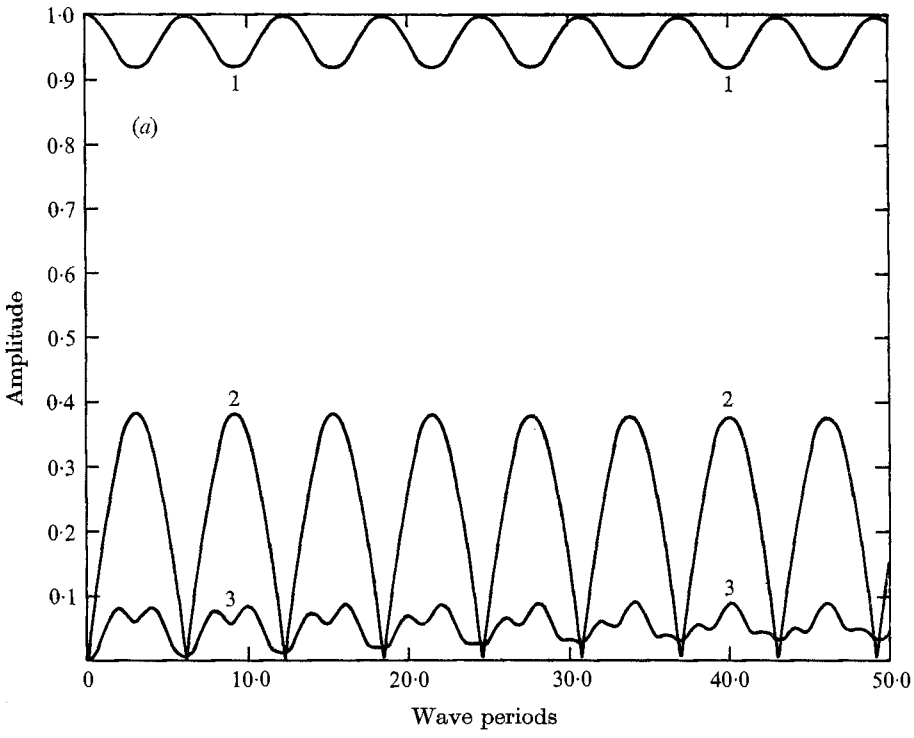

FIGURE 3(*a*). For legend see facing page.

solution are drawn in figure 3(*a*), and the μ-exact solution relative to a frame of reference moving with unit velocity is shown in figure 3(*b*). The figure can be viewed as a perspective drawing of the surface $\eta(x, t)$ relative to the moving frame of reference, with x increasing over 2 wavelengths to the right and t increasing over 50 wave periods away from the viewer. The major ridges are the paths of the crests of the primary wave trains, and the spurs on the sides of the ridges are the paths of the crests of the secondary wave trains.†

When the analytical solution of $\mathscr{S}_3$ derived from (5.5) and (5.7) is compared with the numerical solution, A_1 and A_2 are almost identical, while A_3 differs by only 2 % in magnitude near the end of the range of integration.

$$\epsilon = \tfrac{1}{20}, \quad \mu^2 = \tfrac{1}{10}, \quad \epsilon/\mu^2 = \tfrac{1}{2}$$

The number of harmonics in the Fourier series is 5, 5 or 6; the period of $|A_1|$ is 8·2, 8·8 or 9·4 wave periods; the maximum value of $|A_2|$ is 0·58, 0·58 or 0·60; the phase velocity of the primary wave trains is 0·98 in each case between phase discontinuities at their intersections with the secondary wave trains; and the phase velocity of the secondary wave trains is 0·88 in each case with no measurable phase discontinuities at their intersections with the primary wave trains.

† Individual profiles of η at given t for possible comparison with experiment are available from the author.

(*b*)

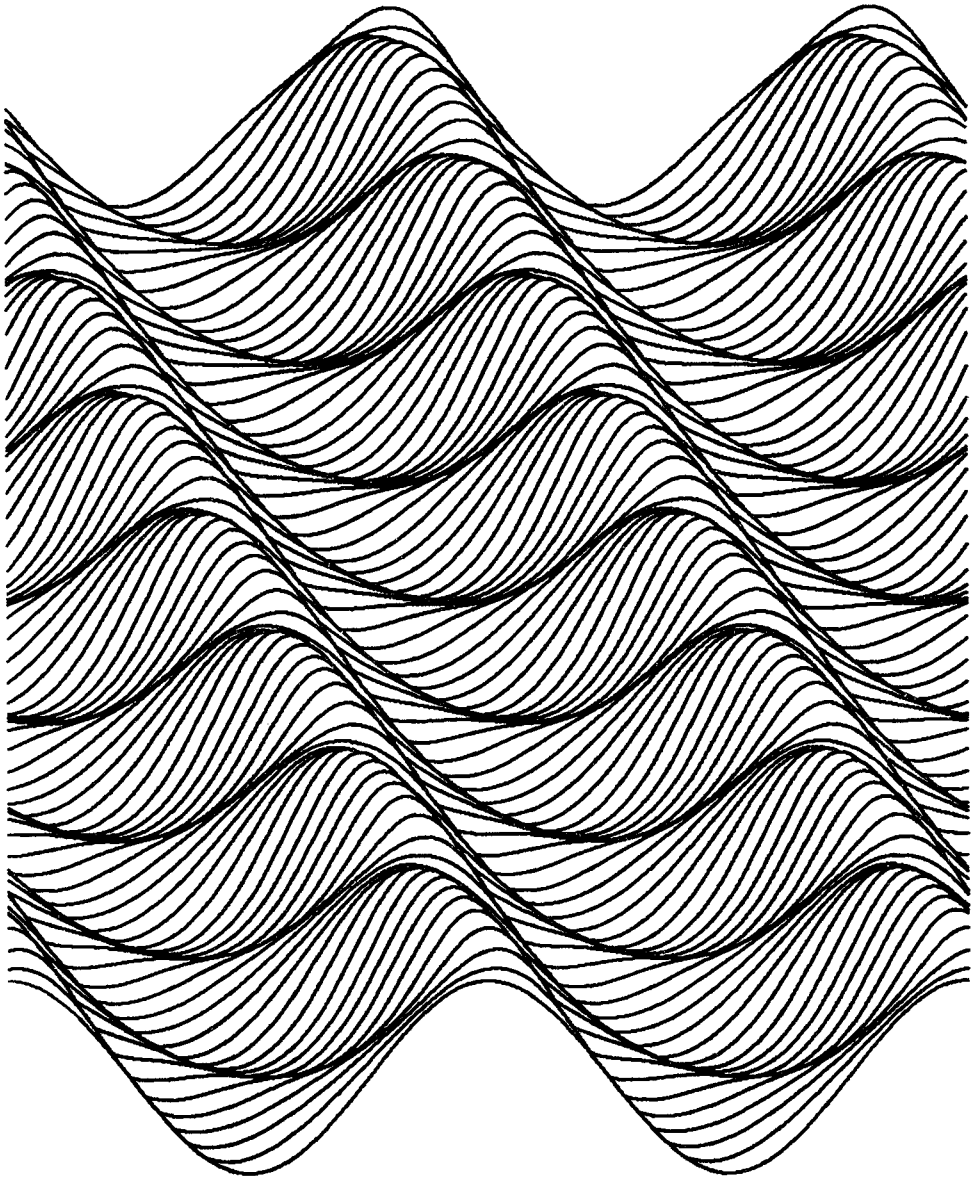

FIGURE 3. $\epsilon = 0{\cdot}05$, $\mu = \sqrt{0{\cdot}2}$. (*a*) $|A_1|$, $|A_2|$, $|A_3|$ from the μ-exact solution. The numbers on the figure refer to the three harmonics. (*b*) The μ-exact solution for $\eta(x, t)$ relative to a frame of reference moving with unit velocity. The lines are graphs of $\eta(x, t)$ at values of t a half wave period apart, from zero to 50 wave periods. Successive graphs are displaced vertically by a constant amount, with any part of a graph that lies below a previous graph being drawn on top of the previous graph.

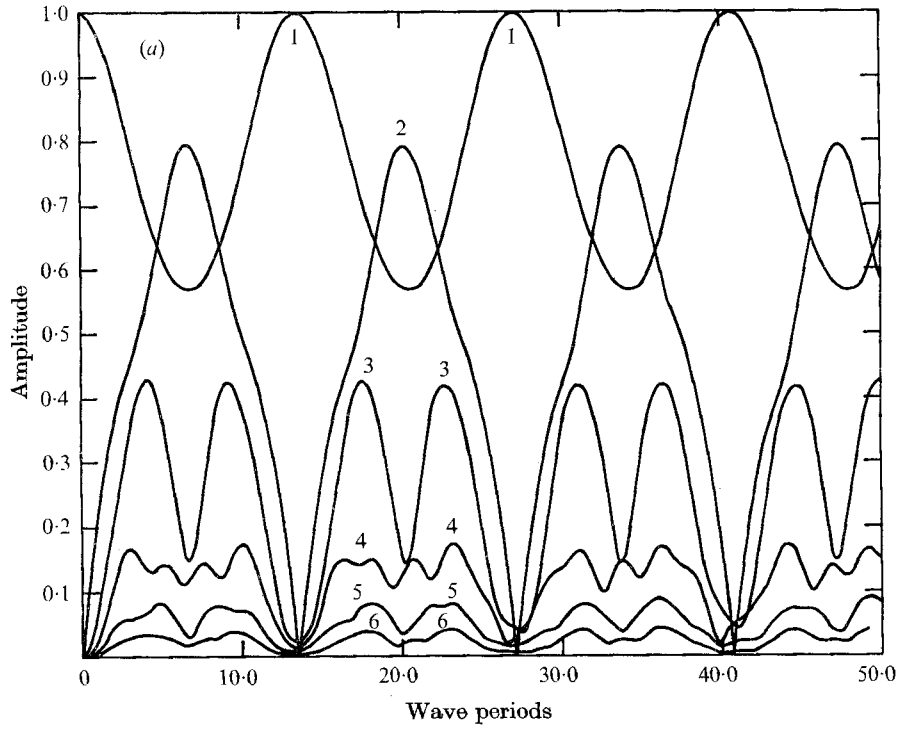

FIGURE 4(*a*). For legend see facing page.

$$\epsilon = \tfrac{1}{20}, \quad \mu^2 = \tfrac{1}{20}, \quad \epsilon/\mu^2 = 1$$

The number of harmonics in the Fourier series is 7, 7 or 8; the period of $|A_1|$ is 12·85, 13·1 or 13·6 wave periods; the maximum value of $|A_2|$ is 0·79, 0·78 or 0·79; the phase velocity of the primary wave trains is 0·998 in each case between discontinuities at their intersections with the secondary wave trains; and the phase velocity of the secondary wave trains is 0·94 in each case between small discontinuities at their intersections with the primary wave trains. The μ-exact amplitudes $|A_1|, \ldots, |A_6|$ are shown in figure 4 (*a*), and the μ-exact solution relative to a frame of reference moving with unit velocity is drawn in figure 4 (*b*). The figure can be viewed as a perspective drawing of the surface $\eta(x, t)$ relative to the moving frame of reference. The major ridges are the paths of the crests of the primary wave trains. Their phase velocity between intersections is seen to be slightly less than 1, even though their overall mean phase velocity exceeds 1. The minor ridges are the paths of the crests of the secondary wave trains. The tertiary wave trains are just discernible as spurs on the sides of the major ridges.

$$\epsilon = \tfrac{1}{20}, \quad \mu^2 = \tfrac{1}{40}, \quad \epsilon/\mu^2 = 2$$

The number of harmonics in the Fourier series is 10, 10 or 11; the period of $|A_1|$ is 18·4, 18·8 or 19·45 wave periods; the maximum value of $|A_2|$ is 0·90, 0·89 or 0·90; the phase velocity of the primary wave trains is 1·002 in each case between phase discontinuities at their intersections with the secondary wave trains and

(*b*)

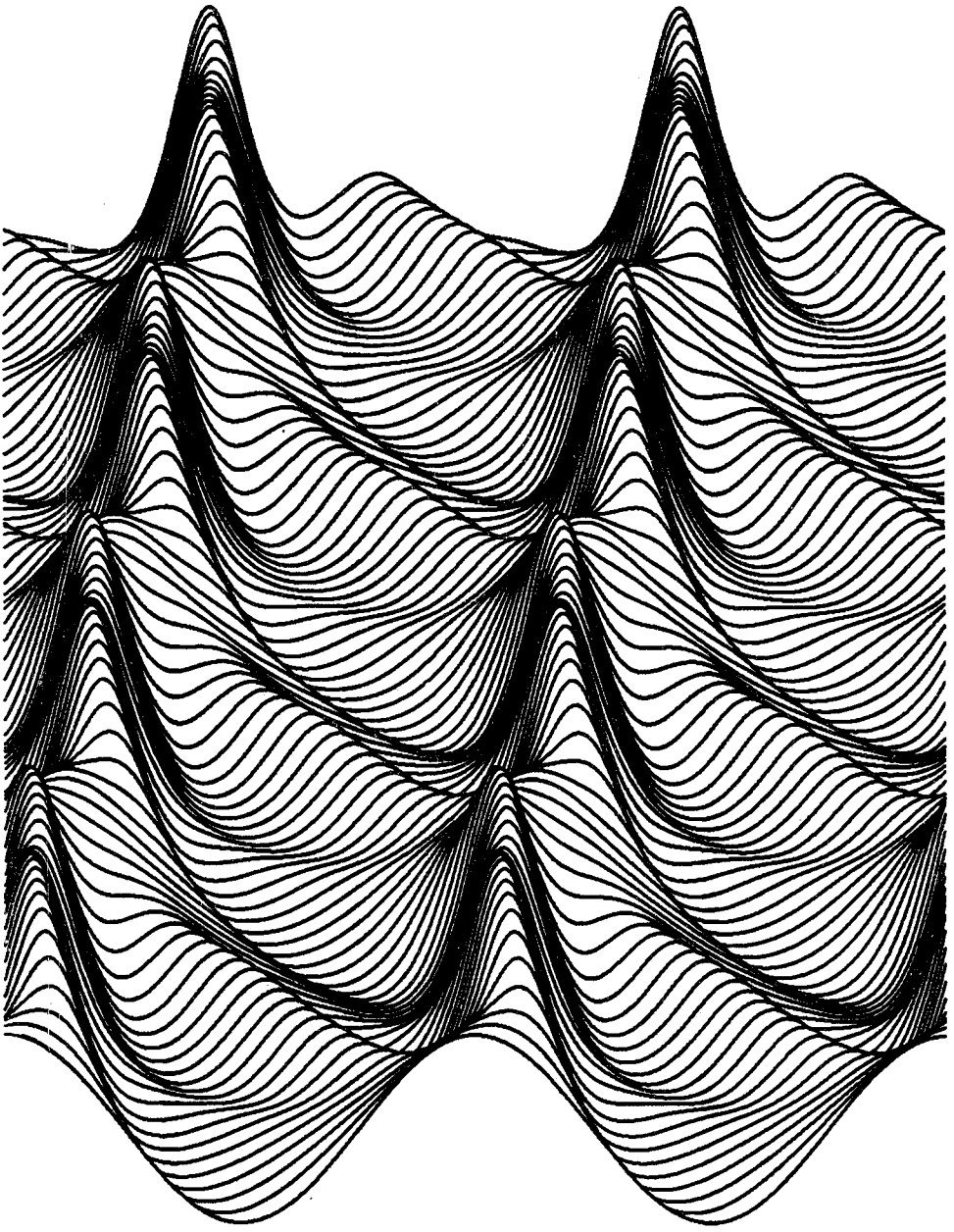

FIGURE 4. $\epsilon = 0{\cdot}05$, $\mu = \sqrt{0{\cdot}05}$. (*a*) $|A_1|, |A_2|, \ldots, |A_6|$ from the μ-exact solution. The numbers on the figure refer to the six harmonics. (*b*) The μ-exact solution for $\eta(x, t)$ relative to a frame of reference moving with unit velocity, plotted as in figure 3 (*b*).

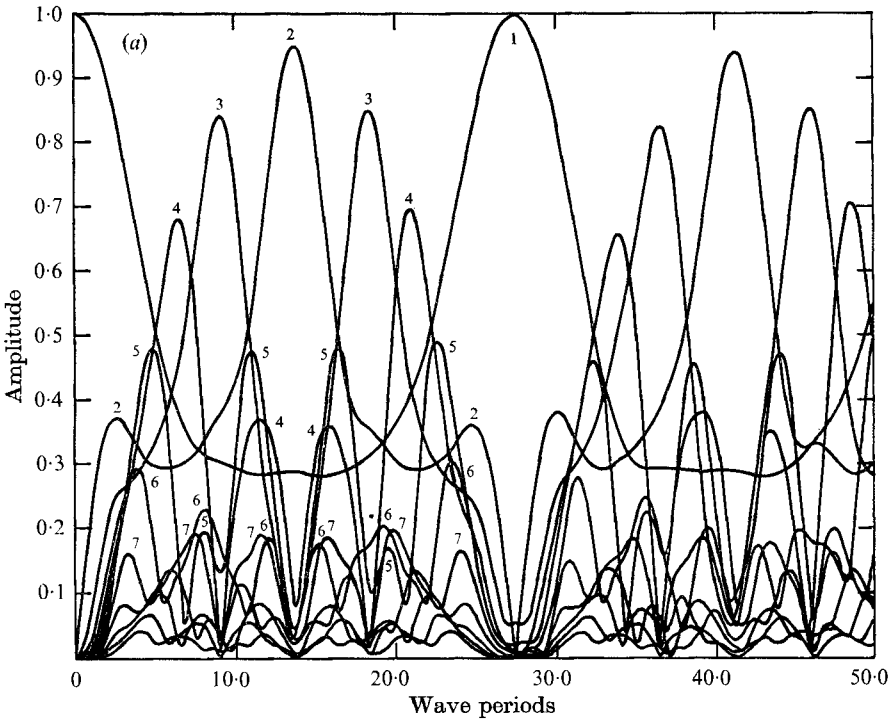

FIGURE 5(*a*). For legend see facing page.

with the tertiary wave trains; the phase velocity of the secondary wave trains is 0·965 in each case between discontinuities at their intersections with the primary wave trains; and the phase velocity of the tertiary wave trains is 0·92 in each case with no measurable discontinuities at their intersections with the primary and secondary wave trains.

$$\epsilon = \tfrac{1}{20}, \quad \mu^2 = \tfrac{1}{30}, \quad \epsilon/\mu^2 = 4$$

The number of harmonics in the Fourier series is 15, 15 or 16; the period of $|A_1|$ is 26·2, 26·85 or 27·65 wave periods; the maximum value of $|A_2|$ is 0·94, 0·95 or 0·95; the phase velocity of the primary wave trains is 1·005 between phase discontinuities; the phase velocity of the secondary wave trains is 0·985 between discontinuities; the phase velocity of the tertiary wave trains is 0·955 between discontinuities; and the phase velocity of the quaternary wave trains is 0·925 without discontinuities. The amplitudes $|A_1|, \ldots, |A_{11}|$ for the μ-exact solution are plotted in figure 5(*a*), and the μ-exact solution relative to a frame of reference moving with unit velocity is shown in figure 5(*b*). The figure can be viewed as a perspective drawing of the surface $\eta(x,t)$ relative to the moving frame of reference. The major ridges are the paths of the crests of the primary wave trains. Each saddle along the major ridges is the region of intersection of a primary wave train with a higher order wave train. Using the saddles as starting points, the paths of the crests of the secondary, tertiary and quaternary wave trains may be followed.

(*b*)

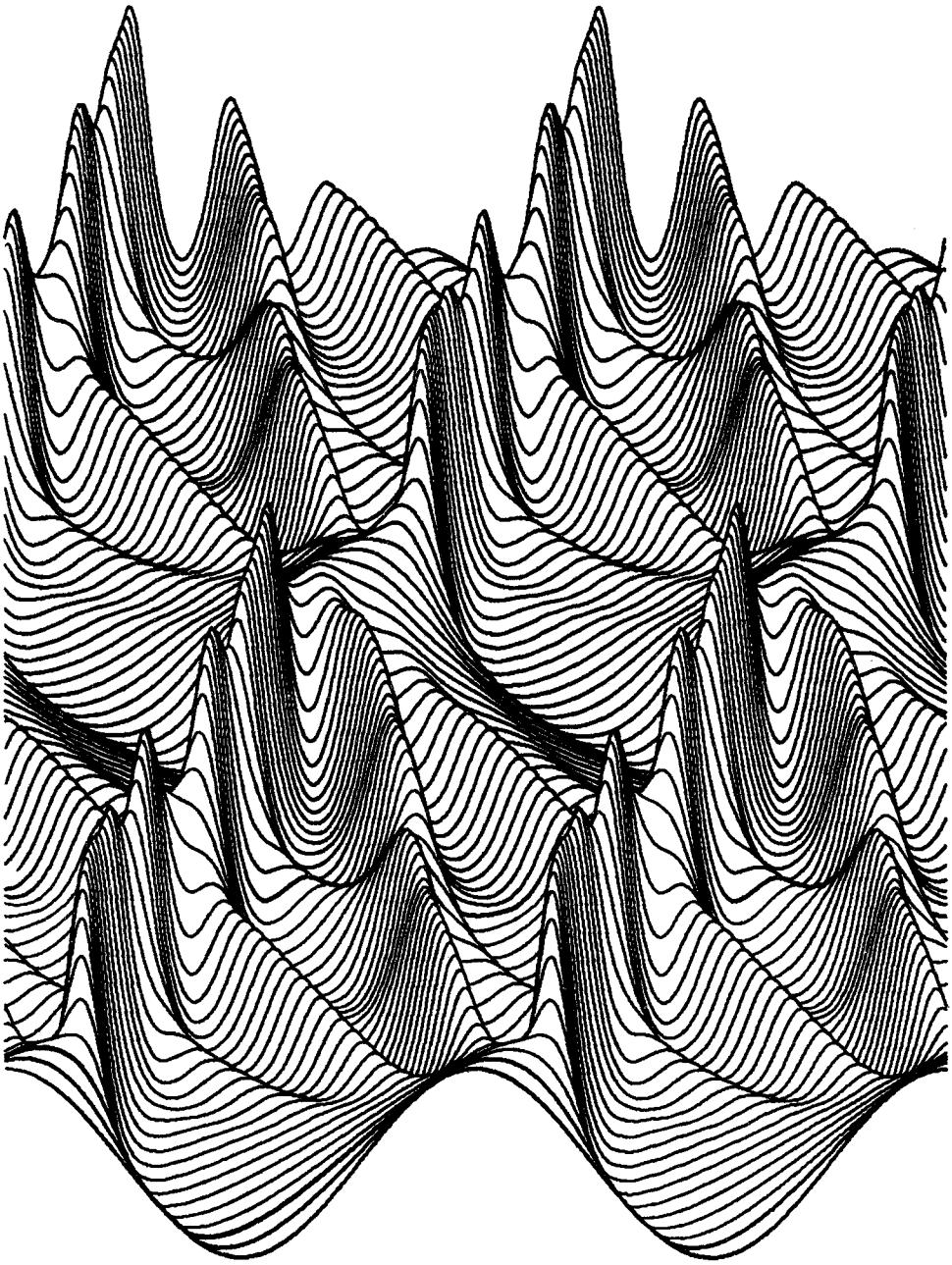

FIGURE 5. $\epsilon = 0{\cdot}05$, $\mu = \sqrt{0{\cdot}0125}$. (*a*) $|A_1|, |A_2|, \ldots, |A_{11}|$ from the μ-exact solution. The numbers on the figure refer to the first seven harmonics. (*b*) The μ-exact solution for $\eta(x, t)$ relative to a frame of reference moving with unit velocity, plotted as in figure 3 (*b*).

$$\epsilon = \tfrac{1}{15}, \quad \mu = \pi\sqrt{0{\cdot}06}, \quad \epsilon/\mu^2 \doteq 0{\cdot}11 \quad (\textit{Vliegenthart } 1971)$$

The range of integration is $0 \leqslant \epsilon t \leqslant 5\pi$, that is, $37\frac{1}{2}$ wave periods from the initial instant. The number of harmonics in the Fourier series is 3, 3 or 4; the period of $|A_1|$ is 1·69, 2·55 or 3·37 wave periods; the maximum value of $|A_2|$ is 0·17, 0·18 or 0·24; and the phase velocity of the primary wave trains is 0·85, 0·89 or 0·89 between phase discontinuities at their intersections with the secondary wave trains. The secondary wave trains are not defined sufficiently clearly to measure their phase velocity.

When the analytical solution of $\mathscr{S}_3$ derived from (5.5) and (5.7) is compared with the numerical solution, the difference is less than 1 % over the whole range of integration.

Vliegenthart presented a numerical solution of the KdV equation over 1·84 wave periods, which he found to be the time taken for the initial profile to be present again, apart from a phase shift. This time, interpreted as the period of both $|A_1|$ and $|A_2|$, is an overestimate by 9 % of the period calculated from (5.7) with the KdV coefficients. Vliegenthart used a spatial increment of $\Delta x = \frac{1}{10}\pi$ (in the present notation) in order to stabilize his numerical scheme. The changes in phase of the first, second and third harmonics across this increment are $\frac{1}{10}\pi$, $\frac{1}{5}\pi$ and $\frac{3}{10}\pi$, respectively. The error in Vliegenthart's scheme is possibly due therefore to the large size of the increment. (The KdV model is well in error anyway at this value of μ.)

$$\epsilon = \tfrac{1}{4}, \quad \mu = \tfrac{1}{8}\pi, \quad \epsilon/\mu^2 = 16/\pi^2 \quad (\textit{Madsen, Mei \& Savage } 1970)$$

This example was not examined with much enthusiasm because the value of ϵ is sufficiently large that approximations made in the derivation of the equations become doubtful. The range of integration is $0 \leqslant \epsilon t \leqslant 5\pi$, that is, 10 wave periods from the initial instant. The Fourier series for the KdV and BBM equations converge sufficiently strongly to be terminated at 10 harmonics. The Fourier series for the μ-exact equations did not converge within the criteria set in § 6, so no values are quoted for the parameters derived with the μ-exact coefficients. The period of $|A_1|$ is 3·3 or 3·75 wave periods; the maximum value of $|A_2|$ is 0·87 or 0·82; the phase velocity of the primary wave trains is 1·00 in both cases between phase discontinuities; the phase velocity of the secondary wave trains is 0·80 in both cases between discontinuities; and the phase velocity of the tertiary wave trains is 0·5 or 0·6 without discontinuities.

Madsen, Mei & Savage present a numerical solution of the KdV equation in which the phase velocities of the primary and secondary wave trains between intersections are found to be 1·08 and 0·86 respectively. The reason for the discrepancy between their results and the present results is not known. Additional confidence is given to the present results because the BBM solution may be confirmed by using a completely different method of numerical solution. This method uses a numerical algorithm constructed from the integral equation form of the BBM equation (Benjamin, Bona & Mahony, equation (3.1)). The phase velocities and wave minima and maxima calculated from the integral equation agree within 1 % with those calculated from the Fourier series.

8. Discussion

The KdV and BBM models both underestimate the period of $|A_1|$, and hence the interaction time of the intersecting wave trains. They also both underestimate the maximum magnitudes of the harmonics, and hence the magnitudes of the wave maxima and minima. It can be seen from the examples that the BBM model provides a better estimate, in almost every case, than the KdV model.

It is interesting that the phase velocities of the intersecting wave trains calculated from the three models are in such close agreement. One possible reason is that the wave trains all have the wavelength 2π of the lowest harmonic. The phase velocity of the wave trains is therefore strongly dependent on the properties of the lowest harmonic, and these are well represented by all three models.

It can be seen in figures 3(*a*), 4(*a*) and 5(*a*) that the nearly periodic time structure of the solutions persists over the whole of the range of integration. A reason for this property was advanced in § 2, namely that the behaviour of the system is dominated by the near-resonant interactions between the lowest harmonics of the initial sinusoidal wave train. Interactions between higher harmonics are insignificant in comparison because they are further from resonance.

It is premature to identify the intersecting wave trains of the solutions as intersecting cnoidal wave trains, because the amplitude and phase velocity relative to still water of individual wave trains cannot be isolated sufficiently accurately to be compared with the known parameters of individual cnoidal wave trains. The next step planned for extending this investigation will be to examine the properties of intersecting cnoidal wave trains with a view to the possibility that they can be identified with the intersecting wave trains of the present solutions. It may be possible then to determine whether or not there is a class of wave trains, of small but finite amplitude on shallow water, which can be represented as a superposition of cnoidal wave trains of the same wavelength.

I am grateful to the University of Essex for their hospitality. I wish to thank Professor T. Brooke Benjamin for reading this manuscript and for his comments on this work.

REFERENCES

BENJAMIN, T. B., BONA, J. L. & MAHONY, J. L. 1972 On model equations for long waves in nonlinear dispersive systems. *Phil. Trans. Roy. Soc.* A **272**, 47.

BONA, J. L. & BRYANT, P. J. 1973 A mathematical model for long waves generated by wavemakers on nonlinear dispersive systems. *Proc. Camb. Phil. Soc.* **73**, 391.

KIM, Y. K. & HANRATTY, T. J. 1971 Weak quadratic interactions of two-dimensional waves. *J. Fluid Mech.* **50**, 107.

KORTEWEG, D. J. & DE VRIES, G. 1895 On the change in form of long waves advancing in a rectangular channel, and on a new type of long stationary waves. *Phil. Mag.* **39**, 422.

MADSEN, O. S., MEI, C. C. & SAVAGE, R. P. 1970 The evolution of time-periodic long waves of finite amplitude. *J. Fluid Mech.* **44**, 195.

VLIEGENTHART, A. C. 1971 On finite-difference methods for the Korteweg–de Vries equation. *J. Engng Math.* **5**, 137.

ZABUSKY, N. J. & GALVIN, C. J. 1971 Shallow-water waves, the Korteweg–de Vries equation and solitons. *J. Fluid Mech.* **47**, 811.